

Springer Monographs in Mathematics

For further volumes published in this series,
www.springer.com/series/3733

Johannes J. Duistermaat

Discrete Integrable Systems

QRT Maps and Elliptic Surfaces

 Springer

Johannes J. Duistermaat (deceased, March 2010)

ISSN 1439-7382

ISBN 978-1-4419-7116-6

e-ISBN 978-0-387-72923-7

DOI 10.1007/978-0-387-72923-7

Springer New York Dordrecht Heidelberg London

Library of Congress Control Number: 2010934229

© Springer Science+Business Media, LLC 2010

All rights reserved. This work may not be translated or copied in whole or in part without the written permission of the publisher (Springer Science+Business Media, LLC, 233 Spring Street, New York, NY 10013, USA), except for brief excerpts in connection with reviews or scholarly analysis. Use in connection with any form of information storage and retrieval, electronic adaptation, computer software, or by similar or dissimilar methodology now known or hereafter developed is forbidden.

The use in this publication of trade names, trademarks, service marks, and similar terms, even if they are not identified as such, is not to be taken as an expression of opinion as to whether or not they are subject to proprietary rights.

Printed on acid-free paper

Springer is part of Springer Science+Business Media (www.springer.com)

Contents

Preface	vii
1 The QRT Map	1
1.1 The Rational Formula for the QRT Map	1
1.2 Indeterminacy of the QRT Map	3
1.3 Reconstruction	4
2 The Pencil of Biquadratic Curves in $\mathbb{P}^1 \times \mathbb{P}^1$	9
2.1 Complex Analytic Geometry	10
2.2 Complex Projective Varieties	28
2.3 Elliptic Curves	33
2.4 Biquadratic Curves	49
2.5 The QRT Mapping on a Smooth Biquadratic Curve	60
2.6 Real Points	74
3 The QRT surface	85
3.1 The surface in $\mathbb{P}^1 \times (\mathbb{P}^1 \times \mathbb{P}^1)$	86
3.2 Blowing Up	93
3.3 Blowing Up $\mathbb{P}^1 \times \mathbb{P}^1$ at the Base Points	105
3.4 The QRT Map on the QRT Surface	119
4 Cubic Curves in the Projective Plane	129
4.1 From $\mathbb{P}^1 \times \mathbb{P}^1$ to \mathbb{P}^2 and Back	129
4.2 Manin Transformations	134
4.3 Manin QRT Automorphisms	138
4.4 Aronhold's Invariants	143
4.5 Pencils of Cubic Curves with Only One Base Point	148
5 The Action of the QRT Map on Homology	157
5.1 The Action of the QRT Map on Homology Classes	157
5.2 QRT Transformations of Finite Order	164
6 Elliptic Surfaces	179
6.1 Fibrations	179

6.2	The Singular Fibers	187
6.3	The Weierstrass Model	271
6.4	Kodaira's Classification of Elliptic Surfaces	314
7	Automorphisms of Elliptic Surfaces	329
7.1	The Mordell–Weil Group and the Set of Sections	329
7.2	The Néron–Severi Group	331
7.3	Eichler–Siegel transformations	338
7.4	The Number of Periodic Fibers	342
7.5	The Contributions of the Reducible Fibers	346
7.6	More about the Mordell–Weil lattices	351
7.7	Asymptotics of the k -Periodic Fibers	355
7.8	The Mordell–Weil Group in the Weierstrass Model	369
8	Elliptic Fibrations with a Real Structure	377
8.1	Real Structures and Real Automorphisms	377
8.2	The Real Periods near the Singular Fibers	384
8.3	Hyperbolic and Elliptic I_b , $b > 0$	391
8.4	Singularities of the Real Rotation Function	395
8.5	Real Pencils	400
9	Rational elliptic surfaces	405
9.1	Equivalent Characterizations of Rational Elliptic Surfaces	405
9.2	Properties of Rational Elliptic Surfaces	410
10	Symmetric QRT Maps	451
10.1	The QRT Root	452
10.2	Pencils of Planar Quadrics	460
10.3	Poncelet	467
11	Examples from the Literature	475
11.1	Hesse	475
11.2	The Elliptic Billiard	487
11.3	The Planar Four-Bar Link	512
11.4	The Lyness Map	518
11.5	The McMillan Map	546
11.6	Heisenberg Spin Chain Maps	553
11.7	The Sine–Gordon map	556
11.8	Jogia's Example	572
11.9	A Non-QRT Map with the Weierstrass Data of a QRT Map	577
12	Appendices	591
12.1	The QRT Mapping on Singular Fibers	591
12.2	Configurations of Singular Fibers in this Book	608
	References	613
	Index	621

Preface

In December 2005, Theo Tuwankotta showed me a birational transformation of the plane derived from a discrete sine-Gordon equation, with the question to determine the behavior of the discrete dynamical system defined by the iterates of the map. The map belongs to the family of QRT maps, introduced in 1988 by Quispel, Roberts, and Thompson, with many examples coming from mathematical physics. Classical examples of QRT maps are the transformations in the theorem of Poncelet and the elliptic billiard. The QRT maps can be identified with the automorphisms of rational elliptic surfaces that act as translations on the smooth fibers and map a smooth section to a disjoint one. This characterization leads to very detailed information about the dynamics. For instance, it leads to an explicit formula for the number of fibers on which the transformation is periodic with a given period k , together with an asymptotic description for large k of the set of such fibers. In the real setting, it leads to a detailed qualitative description of the rotation number of the map, as a function of the real parameter which tells to which fiber the map is restricted.

The definition of the QRT maps is so simple that it can be explained to high school students. In contrast, in order to obtain their basic properties, such as their identification with automorphisms of elliptic surfaces, one needs quite a bit of algebraic and complex analytic geometry. I needed to work out many of the proofs in the literature in order to understand these, and subsequently tell the results to the discrete dynamical systems community. It is the purpose of this book to explain not only the basic facts about the QRT maps, but also the background theory of elliptic surfaces on which these are based. The completeness of the treatment hopefully will allow the reader to become familiar with any selected aspect of the story, without having to make an extensive journey through the literature.

Different categories of readers might read the book in different ways. Readers without a background in discrete dynamical systems or algebraic geometry might start with the definition of QRT maps, then read about their basic properties, take the background theory of elliptic surfaces for granted for awhile, and then browse in the chapter “Examples from the Literature” in order to see how the theory can be applied. People from Discrete Integrable Systems might first look at the examples, and then, for the proofs of the statements about these, consult the background theory

in the previous chapters. Readers with a background in algebraic geometry might be interested in Kodaira's theory of elliptic surfaces, and the rich collection of its applications presented here. Future research can be expected in the identification and analysis of other, possibly higher dimensional birational transformations preserving a fibration by elliptic curves, arising from mathematical physics or otherwise. Complex analytic families of QRT maps are such higher dimensional examples, where the problem would be to describe the bifurcations in the configurations of the singular fibers of the rational elliptic surfaces.

Prerequisites for dealing with the book are courses in differential geometry and complex analysis on a graduate level. For those not familiar with algebraic geometry, the summary in this book of the employed facts from that subject should be helpful in understanding the theory of QRT maps and elliptic surfaces.

Summary of This Book

The QRT Map

Let $p(x, y)$ be a polynomial function in two variables that is *biquadratic* in the sense that for each y , the polynomial $x \mapsto p(x, y)$ is of degree two and, for each x , the polynomial $y \mapsto p(x, y)$ is of degree two. If $p(x, y) = a(y)x^2 + b(y)x + c(y)$, then the *horizontal switch* $\iota_1 : (x, y) \mapsto (x', y)$, which switches the two points on the curve $p(x, y) = 0$ with the same y -coordinate, is given by $x' = -x - b(y)/a(y)$. Similarly we have the *vertical switch* ι_2 , which switches the two points on the curve $p = 0$ with the same x -coordinate. The *QRT mapping* on the curve $p = 0$ is defined as the composition $\tau = \iota_2 \circ \iota_1$ of the horizontal switch and the vertical switch on $p = 0$. The horizontal and the vertical switches are *involutions*, transformations ι such that $\iota \circ \iota$ is equal to the identity, or equivalently, ι is bijective and $\iota^{-1} = \iota$.

Figure 1 shows the horizontal switch ι_1 , the vertical switch ι_2 , and the QRT map $\tau = \iota_2 \circ \iota_1$, acting on the Lyness curve $(x + 1)(y + 1)(x + y + a) - zxy = 0$, or equivalently, $(x + 1)(y + 1)(x + y + a)/xy = z$, see (11.4.2), for $a = 0.4$ and $z = 10.58$.

Remark. With this definition of the QRT map on a biquadratic curve in mind, I found it exciting to read the following at the beginning of Cayley [32]: "... a (2, 2) correspondence is such that to any given position of either point there correspond two positions of the other point. . . Or, what is the same thing, if x, y are the parameters which serve to determine the two points, then x, y are connected by an equation of the form $p(x, y) = 0$ where p is of degree two in each of the variables" However, although he came this close, Cayley did not consider the QRT map of the biquadratic curve $p(x, y) = 0$ in [32]. \circlearrowright

If $p^0(x, y)$ and $p^1(x, y)$ are two linearly independent biquadratic polynomials, then each nonzero linear combination $p_{(z_0, z_1)}(x, y) := z_0 p^0(x, y) + z_1 p^1(x, y)$

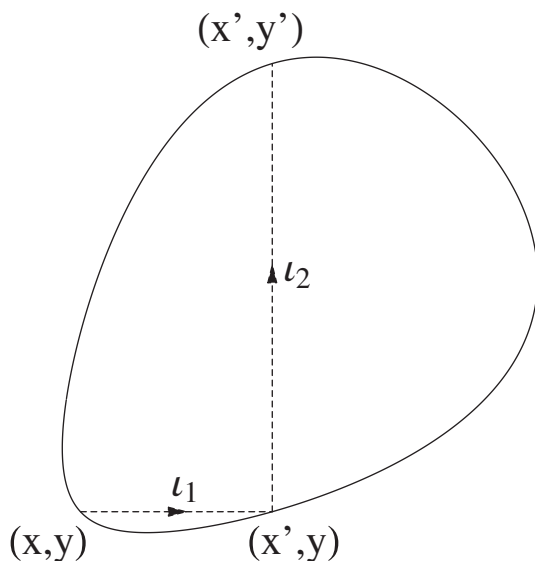


Fig. 1 QRT map on a biquadratic curve.

of p^0 and p^1 is a nonzero biquadratic polynomial. The corresponding biquadratic curve

$$z_0 p^0(x, y) + z_1 p^1(x, y) = 0 \tag{0.0.1}$$

in the (x, y) -plane does not change if both coefficients z_0, z_1 are multiplied by the same factor. Therefore the curves $p_{(z_0, z_1)}(x, y) = 0$ are parametrized by the projective line \mathbb{P}^1 of all one-dimensional linear subspaces of the (z_0, z_1) -plane. Such a one-parameter family of curves in which the parameter z appears linearly in the equations is called a *pencil* of curves.

We have that $p^0(x, y) = 0$ and $p^1(x, y) = 0$ if and only if $p_z(x, y) = 0$ for every z , that is, all the members of the pencil pass through the point (x, y) if and only if two distinct members pass through it. Such a point (x, y) is called a *base point* of the pencil. If we work over the field \mathbb{C} of complex numbers, and projectively, which makes the analysis more uniform, then every pencil of biquadratic curves has eight base points, when counted with multiplicities. On the other hand, if (x, y) is not a base point, then the set of all z such that $p_z(x, y) = 0$ is a one-dimensional linear subspace of the (z_0, z_1) -plane, that is, exactly one member $C = C(x, y)$ of the pencil passes through the point (x, y) . See Figure 3.1.1 for a case in which all eight base points are real and simple, whereas Figure 3.1.2 illustrates a base point of multiplicity two.

It is customary to write $z_0 = 1$ and $z_1 = -z$ when in the complement of the base points the equation (0.0.1) is equivalent to

$$z = p^0(x, y)/p^1(x, y). \tag{0.0.2}$$

That is, the biquadratic curve is equal to the level curve of the rational function p^0/p^1 at the level z . If we apply to (x, y) not a base point the transformations ι_1, ι_2 , and τ of the biquadratic curve $C(x, y)$, then we obtain birational transformations of the plane $\mathbb{P}^1 \times \mathbb{P}^1$. Here the “bi” in birational refers to the fact that both the map and its inverse are rational. These are the birational transformations of the plane that have been introduced, in this generality, by Quispel, Roberts, and Thompson in [168], [169].

The horizontal and vertical switches and the QRT map are, as birational transformations of the plane, explicitly given by the formulas (1.1.4), (1.1.5), (1.1.6). From the way these have been introduced here, it follows that ι_1, ι_2 , and τ , where defined, leave each member of the pencil of biquadratic curves invariant. In Section 2.5 we prove that every smooth member of the pencil is an *elliptic curve*, on which, moreover, the QRT map acts as a *translation*. One proof uses Hamiltonian vector fields tangent to the biquadratic curves that are invariant under the QRT map, and therefore the QRT map acts as a translation in the time parameter of the solution curve of the Hamiltonian system.

The theory in this book will lead to quite detailed information about the behavior of the iterates τ^k of the QRT map τ for large k . I would like to emphasize here that although the formulas for the rational transformations τ^k in principle can be computed successively in an explicit manner, these formulas rapidly become very complicated. In fact, none of the general facts about the QRT maps has been obtained by direct inspection of the formulas for their iterates.

Figure 2 shows the orbit of a point under five iterates of the QRT map of Figure 1.

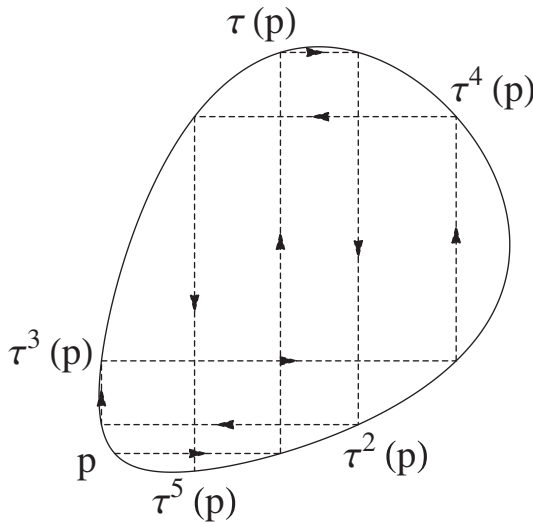


Fig. 2 Five iterates of the QRT map of Figure 1.

Because in the examples one is often interested in real QRT maps, acting as translations on real closed curves, much attention has been paid to the real rotation number, as a function of the real parameter that tells on which curve the QRT map is acting. See Section 2.6 and Chapter 8. Most of the information is obtained by viewing the real curves as the real parts of the complex curves, where it would have been difficult to understand the situation by staying exclusively in the real domain.

Very useful for computations are the formulas for the Weierstrass invariants g_2 , g_3 , and Δ of the biquadratic curves, and the coordinates X and Y of the image point on the Weierstrass curve under the QRT map of the point at infinity on the Weierstrass curve. In fact, X , Y , and g_2 are the basic polynomial invariants of the biquadratic polynomials that define the QRT map. See Corollary 2.4.7 and Proposition 2.5.6. For the QRT root in the case of a pencil of symmetric biquadratic curves, see Proposition 10.1.6. This leads also to an explicit determination of the inhomogeneous Picard–Fuchs equation of the QRT map, and the Beukers–Cushman monotonicity criterion for the rotation function; see Sections 2.5.3 and 2.6.3.

Singularity confinement by Blowing Up

The ambiguity at the base points of the QRT map and its invariant rational function p^0/p^1 , and the phenomenon that all the invariant biquadratic curves in the pencil meet at each base point, can be removed by *blowing up* the plane at the base points. If a base point has multiplicity > 1 , then in the blown-up surface a new base point will appear of multiplicity one less, which then has to be blown up again. As there are eight base points when counted with multiplicity, the process will stop after eight blowing-up transformations. We arrive at a smooth surface, a complex two-dimensional compact, connected complex analytic manifold S , on which the proper transforms of the biquadratic curves of the pencil have become disjoint, where the smooth ones are elliptic curves. The invariant rational function p^0/p^1 corresponds to an everywhere defined complex analytic mapping $\kappa : S \rightarrow \mathbb{P}^1$, of which the fibers are aforementioned proper images of the biquadratic curves, which is why κ is called an *elliptic fibration* of the surface S over the complex projective line. See Definition 6.1.7. Furthermore, the translations on the smooth fibers of S defined by the QRT map τ extend to an *automorphism* τ^S of S , an everywhere defined complex analytic diffeomorphism from S onto itself, without any ambiguities or singularities. More precisely, τ^S belongs to the group $\text{Aut}(S)_\kappa^+$ of all automorphisms of S that preserve each of the fibers of κ and act as a translation on each smooth fiber, which is an elliptic curve. See Section 3.4.2.

It is a basic fact that the biquadratic polynomials on $\mathbb{C}^2 \times \mathbb{C}^2$ correspond bijectively to the holomorphic exterior two-vector fields on $\mathbb{P}^1 \times \mathbb{P}^1$, that is, the holomorphic sections of the anticanonical bundle of $\mathbb{P}^1 \times \mathbb{P}^1$. See Section 2.1.7 for the definition of the anticanonical bundle. Therefore the two-dimensional vector space of biquadratic polynomials that define the pencil of biquadratic curves corresponds to a two-dimensional vector space of holomorphic exterior two-vector fields on $\mathbb{P}^1 \times \mathbb{P}^1$,

and at each blowing up we have a corresponding two-dimensional vector space of holomorphic exterior two-vector fields on the blown-up surface. When we arrive at our surface S , the two-dimensional vector space of holomorphic exterior two-vector fields is equal to the space of *all* holomorphic exterior two-vector fields on S , where the fibers of κ are precisely the zero-sets of the nonzero holomorphic exterior two-vector fields on S . Actually, we use the two-dimensional vector spaces of holomorphic vector fields in order to find the base points in an intermediate blown up surface, which may occur over base points of higher multiplicity of the pencil of biquadratic curves in $\mathbb{P}^1 \times \mathbb{P}^1$. See Section 3.3.2–3.3.4.

Automorphisms of Rational Elliptic Surfaces

Blowing up one base point b of the pencil of biquadratic curves and then blowing down the proper transforms of the horizontal and vertical axes through b , we arrive at the complex projective plane \mathbb{P}^2 , in which the pencil of biquadratic curves corresponds to a pencil of cubic curves, with the respective blowdowns b_1 and b_2 of the horizontal and vertical axis as two of its base points. Conversely, every pencil of cubic curves in \mathbb{P}^2 with at least two base points arises in this way.

Every complex projective line in \mathbb{P}^2 intersects a cubic curve in three points. The horizontal or vertical switch on the biquadratic curve corresponds to the mapping ι_{C, b_2} or ι_{C, b_1} , which assigns to the point x on the cubic curve C the third point of intersection with C of the complex projective line through x and b_2 or b_1 , respectively. Every smooth cubic curve C in \mathbb{P}^2 is an elliptic curve, and the composition $\tau_{C, b_1} = \iota_{C, b_1} \circ \iota_{C, b_1}$ of these two involutions, which corresponds to the QRT map on the biquadratic curve in $\mathbb{P}^1 \times \mathbb{P}^1$, is equal to the unique translation on C that maps b_1 to b_2 . Doing this for all members of the pencil of cubic curves with the given base points b_1 and b_2 , we obtain a birational transformation of the projective plane \mathbb{P}^2 .

It follows from the theorem of Bézout that every pencil of cubic curves in \mathbb{P}^2 has $3 \times 3 = 9$ base points, when counted with multiplicities. Blowing up the base points in the same way as for our pencil of biquadratic curves in $\mathbb{P}^1 \times \mathbb{P}^1$, we arrive at a surface S in which the pencil of cubic curves corresponds to fibration, where the smooth fibers are elliptic curves, and the rational transformation of \mathbb{P}^2 corresponds to an automorphism of S that acts as a translation on each smooth fiber. These automorphisms of S , defined for each choice of two distinct base points of the given pencil of cubic curves in \mathbb{P}^2 , were introduced by Manin [129, p. 95, 96].

The elliptic surface that is obtained by blowing up the base points of the pencil of cubic curves in \mathbb{P}^2 is canonically isomorphic to the surface obtained by blowing up the pencil of biquadratic curves in $\mathbb{P}^1 \times \mathbb{P}^1$ if the pencil of cubic curves in \mathbb{P}^2 corresponds to the pencil of biquadratic curves in $\mathbb{P}^1 \times \mathbb{P}^1$ as described above. Furthermore, the isomorphism conjugates the QRT automorphism with the Manin automorphism. In this sense the QRT automorphisms and the Manin automorphisms are the same.

In general, the elliptic surfaces that are isomorphic to the blowing up of the base points of a pencil of cubic curves in \mathbb{P}^2 are called *rational elliptic surfaces*. Note

that the rational elliptic surfaces obtained by blowing up the base points of a given pencil of cubic curves in \mathbb{P}^2 are unique up to isomorphism, but that very different pencils of cubic curves in \mathbb{P}^2 can give rise to isomorphic rational elliptic surfaces. See Theorem 4.3.2, Theorem 4.3.3, and Remark 9.2.28.

Each rational elliptic surface has at least one section, for instance the -1 curve that appeared at the last blowing up. If $\varphi : S \rightarrow C$ is any elliptic fibration over a curve C , then the group of all automorphisms of S that act on each smooth fiber φ as a translation will be denoted by $\text{Aut}(S)_\varphi^+$. Here the plus sign refers to the convention to view the composition in a translation group as an addition. If φ has at least one section, then the group $\text{Aut}(S)_\varphi^+$ acts freely and transitively on the set Σ of all sections of φ ; see Lemma 7.1.1. That is, after the choice of a holomorphic section as the “zero section,” the set Σ is identified with the group $\text{Aut}(S)_\varphi^+$, and the set of all sections provided with such a group structure is called the *Mordell–Weil group* of S in the literature. Because we are primarily interested in the group $\text{Aut}(S)_\varphi^+$, and have no canonical choice of a holomorphic section, we prefer to call $\text{Aut}(S)_\varphi^+$ the Mordell–Weil group.

The identification of the QRT automorphisms of the rational elliptic surface S with the corresponding Manin automorphisms allows us to characterize the QRT automorphisms as those elements of the Mordell–Weil group of S that map some (every) section to a disjoint one. Because a theorem of Oguiso and Shioda [155, Theorem 2.5] says that the Mordell–Weil group is generated by elements that map a holomorphic section to a disjoint one, it follows that the Manin QRT automorphisms generate the Mordell–Weil group of S ; see Theorem 4.3.3.

Action on Homology Classes and the Number of k -Periodic Fibers

The -1 curves that appear at each blowing up define real two-dimensional cycles in the rational elliptic surface S . The homology classes of these cycles are independent in the homology group $H_2(S, \mathbb{Z})$ of S . Since $H_2(\mathbb{P}^1 \times \mathbb{P}^1, \mathbb{Z}) \simeq \mathbb{Z}^2$, it follows that $H_2(S, \mathbb{Z}) \simeq \mathbb{Z}^{10}$. Each automorphism of S induces an automorphism of the group $H_2(S, \mathbb{Z})$ that preserves the intersection form on $H_2(S, \mathbb{Z})$. It turns out that the actions on $H_2(S, \mathbb{Z})$ of the elements of the Mordell–Weil group are of a very special nature. In Section 5.1 we determine the action on $H_2(S, \mathbb{Z})$ of the QRT automorphism, under the assumption that no member of the pencil of biquadratic curves contains a horizontal or a vertical axis. See Corollary 5.1.9.

Let $\varphi : S \rightarrow C$ be an elliptic fibration with at least one section E , and let $\alpha \in \text{Aut}(S)_\varphi^+$. If S^{reg} denotes the set of regular points in S , then E intersects each fiber F in exactly one point $s \in F \cap S^{\text{reg}}$, where the intersection is transversal. We have that $\alpha(E)$ intersects E at $s \in F$ if and only if $\alpha(s) = s$ if and only if $\alpha(f) = f$ for every $f \in F$. For this reason the topological intersection number $\nu(\alpha) = E \cdot \alpha(E)$ of the cycles E and $\alpha(E)$ is called the *number of fixed point fibers for α , counted with multiplicities*. This number is independent of the choice of the section. For any $k \in \mathbb{Z}$, the number $\nu(\alpha^k)$ is called the *number of k -periodic fibers for α , counted with multiplicities*. See Definitions 7.4.3 and 7.4.5 for more details.

Because the topological intersection number is a homology invariant, see Section 2.1.6, the numbers $\nu(\alpha^k)$ can be computed in terms of the action of α on $H_2(S, \mathbb{Z})$. In this way we obtain that the number of k -periodic fibers for the QRT automorphism, counted with multiplicities, is equal to $k^2 - 1$ if no member of the pencil of biquadratic curves contains a horizontal or a vertical axis. If at least one member of the pencil of biquadratic curves contains a horizontal or a vertical axis, then there is at least one singular fiber F of the fibration $\kappa : S \rightarrow \mathbb{P}^1$ such that the QRT automorphism permutes the irreducible components of F in a nontrivial way. See Corollary 5.1.12. In this case the behavior of the number of k -periodic fibers is more complicated, but still can be determined explicitly if one knows the action on the set of irreducible components of reducible fibers. See (4.3.2).

Periodic QRT Mappings

Let $\kappa : S \rightarrow \mathbb{P}^1$ be a rational elliptic surface, and let α be a nontrivial element of the Mordell–Weil group $\text{Aut}(S)_\kappa^+$ of a finite order m . That is, all fibers of κ are m -periodic for α . Then the theory of Shioda [184] implies that α maps every holomorphic section of κ to a disjoint one, and therefore there is a pencil of biquadratic curves in $\mathbb{P}^1 \times \mathbb{P}^1$ such that S and κ are the corresponding rational elliptic surface and QRT automorphism. The order m of α can be 2, 3, 4, 5, or 6, and in Section 5.2 we give an explicit description of the Weierstrass data of the elements of the Mordell–Weil group of order m , for each $2 \leq m \leq 6$. In order to find pencils of biquadratic curves such that the QRT map is of the given order, we use the criterion of Oguiso and Shioda that α is of finite order if and only if the sum of the so-called contributions to α of all the reducible fibers is equal to two. Then a pencil is constructed with some reducible fibers, of which the irreducible components are permuted by the QRT map in the required fashion. For each of the possible orders 2, 3, 4, 5, 6, Tsuda [196, Example 3.5] provided a family of pencils for which the QRT mapping has the prescribed order, without telling how he found these families.

Elliptic Surfaces

In Chapter 6 we discuss the theory of arbitrary elliptic fibrations. After the basic definition and some preliminary observations in Section 6.1, Kodaira’s classification of the possibilities for the singular fibers appears in Section 6.2.6. Kodaira’s classification of elliptic surfaces in terms of their *modulus function* and *monodromy representation* is presented in Section 6.4.2. The richness of the province of the elliptic surfaces in the realm of the arbitrary surfaces is illustrated by the fact that for any meromorphic function on a compact connected complex analytic curve C there exists at least one elliptic fibration $\varphi : S \rightarrow C$ with a holomorphic section, having the given meromorphic function on C as its modulus function. In order to make the presentation more self-contained, we have included in Chapter 6 full proofs of all the basic facts about elliptic surfaces. Because of the highly nontrivial nature of many of these basic facts, Chapter 6 has grown into a small book within the book.

As for rational elliptic surfaces, the Mordell–Weil group of S is defined as the group $\text{Aut}(S)_\varphi^+$ of all complex analytic diffeomorphisms α of S that act as a translation on each of the smooth fibers S_c of φ , where S_c is an elliptic curve. If $\varphi : S \rightarrow C$ has a holomorphic section, then S is projective algebraic, and it makes sense to define the Néron–Severi group $\text{NS}(S)$ of S as the subgroup of $H_2(S, \mathbb{Z})$ generated by the homology classes of algebraic curves in S . If S is a rational elliptic surface, then $\text{NS}(S) = H_2(S, \mathbb{Z})$, but for general elliptic surfaces the Néron–Severi group can be quite a bit smaller than the homology group. If $\varphi : S \rightarrow C$ has at least one section and at least one singular fiber, then the theory of Shioda [184] about the action of the Mordell–Weil group $\text{Aut}(S)_\varphi^+$ on $\text{NS}(S)$ leads to detailed information about the structure of the Mordell–Weil group. See Section 7.5. It also leads to the explicit formula (7.5.2) for the number of k -periodic fibers for $\alpha \in \text{Aut}(S)_\varphi^+$, counted with multiplicities. In particular, unless α has finite order, the number of k -periodic fibers grows as k^2 as $k \rightarrow \infty$.

This illustrates that the elements of the Mordell–Weil group of an arbitrary elliptic surface share many properties with QRT transformations, the elements of the Mordell–Weil groups of rational elliptic surfaces without fixed point fibers. Since the rational elliptic surfaces form a quite small subclass of elliptic surfaces, in some sense the first nontrivial one in the hierarchy, the elements of Mordell–Weil groups of arbitrary elliptic surfaces can be viewed as a generalization of QRT maps to a large class of transformations that nevertheless have quite similar properties. However, the attractiveness of QRT maps is that many aspects of them, such as their Weierstrass normal forms, are given by explicit formulas, which I do not know of for the elements of the Mordell–Weil groups of arbitrary elliptic surfaces. Moreover, as illustrated by Chapter 11, quite a large number of birational transformations of the plane turn out to be QRT maps, whereas there are not so many explicit examples of Mordell–Weil groups of elliptic surfaces that are not QRT transformations. In this respect, further explorations might lead to future surprises. For an example in the literature of a non-QRT element of a Mordell–Weil group of an elliptic surface, see Section 11.9.1.

Asymptotic Density of the k -Periodic Fibers

The formula for the number of k -periodic fibers is based on quite nontrivial algebraic geometric or algebraic topological facts, but the corollary that, asymptotically for $k \rightarrow \infty$, it is of order k^2 also follows from the following more elementary analysis. If $p_1(c)$ and $p_2(c)$ are two basic complex periods of the Hamiltonian flow on the smooth fiber S_c in S over the point $c \in C$ of $\varphi : S \rightarrow C$, then $(r_1, r_2) \mapsto r_1 p_1(c) + r_2 p_2(c)$ defines an isomorphism of real Lie groups from the two-dimensional standard torus $(\mathbb{R}/\mathbb{Z}) \times (\mathbb{R}/\mathbb{Z})$ onto the group of translations on S_c , where the isomorphism locally can be made to depend in a real analytic fashion on the regular value c of φ . The warning here is that the isomorphisms are determined only up to orientation-preserving automorphisms of $(\mathbb{R}/\mathbb{Z}) \times (\mathbb{R}/\mathbb{Z})$, defined by elements of $\text{SL}(2, \mathbb{Z})$, and have multivalued real analytic continuations to the set C^{reg} of all regular values of φ .

The element $\alpha \in \text{Aut}(S)_\varphi^+$ then corresponds to a multivalued real analytic mapping R from C^{reg} to $(\mathbb{R}/\mathbb{Z}) \times (\mathbb{R}/\mathbb{Z})$, called the *rotation map* defined by α . In the sequel we assume that the rotation map is not constant.

Let C_{α^k} denote the set of all $c \in C$ such that S_c is a k -periodic fiber for α . If $c \in C^{\text{reg}}$, then $c \in C_{\alpha^k}$ if and only if $R(c) = (k_1/k + \mathbb{Z}, k_2/k + \mathbb{Z})$ for some $k_1, k_2 \in \mathbb{Z}/k\mathbb{Z}$. It follows that, asymptotically for $k \rightarrow \infty$ and near a regular point of R , a point $c \in C^{\text{reg}}$ near which R is a local diffeomorphism, the set C_{α^k} looks like a rank two lattice with distances between neighboring points of order $1/k$. Furthermore, the rescaled lattice at the point c is conformal to the period lattice of the elliptic curve S_c . The rotation map has only finitely many singular points in C^{reg} , near which points R behave like a branched covering, and where the asymptotic density of C_{α^k} is of smaller order. Near the singular values in C of φ , the density of C_{α^k} can be of higher order, but it follows from the asymptotics near every point of C that the total number $\#(C_{\alpha^k})$ of all k -periodic fibers remains of order k^2 as $k \rightarrow \infty$. The asymptotic density of C_{α^k} is described by the real-valued two-form $dR_1 \wedge dR_2$ on C^{reg} . This is a *single-valued* real analytic area form on C^{reg} . It is strictly positive at all points except at the finitely many singular points of the rotation mapping, where it is equal to zero. See Lemma 7.7.7, Corollary 7.7.8, and Corollary 7.7.10 for more details.

If all objects are defined over \mathbb{R} , then the real fibers over the real points c in C^{reg} are either empty, isomorphic to a circle \mathbb{R}/\mathbb{Z} , or isomorphic to two such circles. The element $\alpha \in \text{Aut}(S)_\varphi^+$ acts on each circle as a rotation over a number $\rho(c) \in \mathbb{R}/\mathbb{Z}$, unless it permutes two connected components of the real fibers, when α^2 acts as a rotation on the real fiber. We assume that the *rotation function* $\rho : c \mapsto \rho(c)$ is not constant, which is equivalent to the condition that the aforementioned two-dimensional rotation map R is not constant. Asymptotically for $k \rightarrow \infty$ and near the regular points of ρ , the set of all $c \in C^{\text{reg}}(\mathbb{R})$ such that $S_c(\mathbb{R})$ is a k -periodic real fiber looks like a rank-one lattice with distances between neighboring points of order $1/k$. The number of k -periodic real fibers is asymptotically of order k as $k \rightarrow \infty$. However, in contrast to the complex case, we do not have an explicit formula for the number of k -periodic real fibers.

Rational Elliptic Surfaces

Each surface that comes from a pencil of biquadratic curves in $\mathbb{P}^1 \times \mathbb{P}^1$, which is the natural domain of definition of the QRT automorphism, is a rational elliptic surface. The only rational elliptic surfaces $\kappa : S \rightarrow \mathbb{P}^1$ that are not QRT surfaces are those for which the Mordell–Weil group $\text{Aut}(S)_\kappa^+$ is trivial, that is, those that have only one section. There are only two isomorphism classes of such exceptional rational elliptic surfaces, see Corollary 4.5.6.

In Section 9.1 we give a number of equivalent characterizations of rational elliptic surfaces, which might be useful to determine whether a given elliptic fibration is a rational elliptic surface. In Section 9.2 we collect a number of specific properties of rational elliptic surfaces. When dealing with examples, we sometimes refer to the

list of Persson [156, pp. 7–14] of all possible configurations of singular fibers in a rational elliptic surface. In the list of Oguiso and Shioda [155, pp. 84–86], singular fibers have not been distinguished from each other if the intersection diagrams of their irreducible components are the same. On the other hand, the list of Oguiso and Shioda gives more detailed information about the Mordell–Weil group in terms of the intersection form on the homology group $H_2(S, \mathbb{Z})$.

In the province of the elliptic surfaces, the rational elliptic surfaces form a village with a few hundred inhabitants. As a passer-by, I have met many of them. For a full understanding of rational elliptic surfaces one should know them all.

Examples

The interest of the whole subject is greatly enhanced by the large collection of examples that exist in the literature. One common characteristic of these examples is that each one of these exhibits some very special behavior, not at all shown by the “generic” cases. For instance, the configuration of the singular fibers in the examples is never equal to the generic one $12 I_1$, and for the pencils of symmetric biquadratic curves the configuration of the singular fibers in the examples is never equal to the generic one $3 I_2 \ 6 I_1$. This taught me at a very early stage that I should aim at statements that are truly general, that is, not valid only under some genericity assumption.

We begin, in Section 11.1, with the fascinating pencil of cubic curves in the complex projective plane that studied by Hesse [82]. It is characterized by the property that the nine base points of the pencil are precisely the flex points of each of the smooth members of the pencil. By means of a projective linear transformation the pencil can be brought into a normal form that was Hesse’s point of departure. The sections of the corresponding rational elliptic surface $\kappa : S \rightarrow \mathbb{P}^1$ correspond bijectively to the nine base points, and the Mordell–Weil group is isomorphic to $(\mathbb{Z}/3\mathbb{Z}) \times (\mathbb{Z}/3\mathbb{Z})$. Every automorphism of S is induced by a projective linear transformation, and the group of these, which has 216 elements, also was determined by Hesse.

A biquadratic polynomial $p(x, y)$ is called *symmetric* if $p(x, y) = p(y, x)$ for every $x, y \in \mathbb{C}^2$, when the corresponding curve $p(x, y) = 0$ in $\mathbb{P}^1 \times \mathbb{P}^1$ is invariant under the *symmetry switch* $(x, y) \mapsto (y, x)$. The great majority of the examples of QRT maps in the literature turn out to be defined by pencils of symmetric biquadratic curves. The symmetry condition implies that the QRT mapping τ can be written as $\tau = \rho \circ \rho$, where the *QRT root* ρ is defined as the composition of the horizontal switch followed by the symmetry switch. The symmetry condition implies that the QRT surface S has reducible singular fibers of which the irreducible components are permuted in a nontrivial way. In particular, the rank of the Mordell–Weil group of S is at most equal to 5, whereas for the generic rational elliptic surface the rank of the Mordell–Weil group is equal to 8. For the generic symmetric QRT surface the configuration of the singular fibers is $3 I_2 \ 6 I_1$, in contrast to the configuration $12 I_1$ for the generic rational elliptic surface. See Section 10.1 for more details.

In Section 10.2 we show that pencils of symmetric biquadratic curves in $\mathbb{P}^1 \times \mathbb{P}^1$ are in bijective correspondence with pencils of quadrics in \mathbb{P}^2 . In Section 10.3.3 we show that this correspondence conjugates the QRT root with the *Poncelet mapping* for pairs of quadrics, where the inscribed quadric corresponds to the diagonal in $\mathbb{P}^1 \times \mathbb{P}^1$ and the circumscribed quadric belongs to the pencil. Because the QRT root is a translation on each smooth fiber, we thus recover Poncelet's theorem that if a fiber contains a k -periodic point of the Poncelet mapping, then every point of the fiber is k -periodic.

In Section 11.2 we discuss the elliptic billiard. We show that the billiard map is a Poncelet mapping, and therefore a QRT root for a pencil of symmetric biquadratic curves in $\mathbb{P}^1 \times \mathbb{P}^1$, where the pencil of quadrics in \mathbb{P}^2 consists of the duals of the inscribed confocal quadrics for the billiard trajectories. The configuration of the singular fibers of the corresponding rational elliptic surface is $I_0^* 3 I_2$, which illustrates that the billiard map is quite special among the general QRT roots. Another classical example is the *planar four-bar link*, the Darboux transformation of which is a QRT map on a nonsymmetric biquadratic curve. Because classically this example is not treated in the framework of a one-parameter family of elliptic curves, our discussion in Section 11.3 of the four-bar link is relatively short.

A more recent example that has obtained considerable attention in the literature is the Lyness map, which for this reason is discussed in great detail in Section 11.4. Beukers and Cushman [16], using Picard–Fuchs equations, proved the *conjecture of Zeeman* that the rotation function of the Lyness map has no stationary points in a certain interval between singular values of the fibration. Among other things, we determine the qualitative behavior of the rotation function in every such interval, including a description of the changes in the intervals when the parameter a in the Lyness map passes through its bifurcation values.

In the sections 11.5–refsGsec we discuss a number of examples of QRT roots from the mathematical physics literature, namely the KdV, the modified KdV, and the nonlinear Schrödinger maps, all of which are special McMillan maps; the Heisenberg spin chain map; and the sine–Gordon map. The last of these is treated in much detail because it is the one that introduced me to the subject of this book. Chapter 11 is concluded in Section 11.8 with a discussion of Jogia's example, and in Section 11.9 the example of Viallet, Grammaticos, and Ramani of a non-QRT map with the Weierstrass data of a QRT map.

Section 12.1 contains a list of singular fibers that appear after blowing up a singular member of a given pencil of biquadratic curves in $\mathbb{P}^1 \times \mathbb{P}^1$, together with the action of the QRT automorphism on the set of irreducible components of the singular fiber. We have used this in some concrete examples in order to determine how the QRT automorphism permutes the irreducible components of the reducible singular fibers. For future computations it may be useful to have the complete list of Section 12.1.

What May Be New

Most of the facts in this story are known, and I have done my best to give proper references to the literature. However, there are also many results that I did not see in the literature, and might be new. Some of these results are not entirely straightforward applications of the known theory. Below follows a selection.

- The description of the holomorphic tangent vector fields to the smooth biquadratic curves in $\mathbb{P}^1 \times \mathbb{P}^1$ and the smooth cubic curves in \mathbb{P}^2 as Hamiltonian vector fields, in Lemma 2.4.5 and Lemma 4.1.2, respectively. See also Lemma 3.3.4.

For a general elliptic fibration $\varphi : S \rightarrow C$, the holomorphic vector field on the complement of finitely many fibers of an elliptic fibration, which corresponds to a meromorphic section of the Lie algebra bundle \mathfrak{g} over C , can be viewed as a Hamiltonian vector field as in Remark 6.2.21. The elliptic fibration can be viewed as a completely integrable Hamiltonian system; see Remark 6.2.22.

- The identification of the Eisenstein invariants of the partial discriminants of the biquadratic polynomial with the Weierstrass invariants g_2 , g_3 , and Δ of the period lattice of the biquadratic curve in $\mathbb{P}^1 \times \mathbb{P}^1$. The identification of the image point (X, Y) under the QRT transformation of the point at infinity on the Weierstrass curve with the Frobenius invariants of order two and three of the biquadratic polynomial. See Corollary 2.4.7, Proposition 2.5.6, and Remark 2.5.7. For the QRT root in the case of symmetric biquadratic polynomials, see Proposition 10.1.6.
- The identification of the Aronhold invariants of a cubic polynomial with the Weierstrass invariants of the period lattice of the cubic curve. The relation between biquadratic curves in $\mathbb{P}^1 \times \mathbb{P}^1$ and cubic curves in \mathbb{P}^2 leads to corresponding identities between the Eisenstein invariants of the partial discriminants of a biquadratic polynomial and the Aronhold invariants of a cubic polynomial. See Proposition 4.4.3 and Corollary 4.4.7.
- The corresponding morphisms between the various moduli spaces in Subsection 6.3.3.
- The inhomogeneous Picard–Fuchs equation = Manin homomorphism for the element of the Mordell–Weil group of an elliptic fibration, explicitly computable for the QRT map. The generalization to all QRT maps of the Beukers–Cushman criterion for monotonicity of the real period function. See Sections 2.5.3, 7.8, and 2.6.3.
- The characterization in Theorem 4.3.2 of the elements of the Mordell–Weil group of a rational elliptic surface that are QRT automorphisms or Manin automorphisms for a pencil of biquadratic or cubic curves in $\mathbb{P}^1 \times \mathbb{P}^1$ or \mathbb{P}^2 , respectively, where the surface is obtained by successively blowing up the base points of the anticanonical pencils.
- The classification in Section 4.5 of the pencils of cubic curves in \mathbb{P}^2 with only one base point, which therefore has multiplicity 9. These are the pencils that do not have a Manin transformation. This leads to the classification in Corollary 4.5.6 of the rational elliptic surfaces with a trivial Mordell–Weil group.

- The generalization of a large part of Kodaira's theory of elliptic surfaces to the case in which it is allowed that the elliptic surfaces are not compact or that the modulus function is constant.
- The description in Lemma 6.2.38 and Table 6.2.39 of the basis of periods near a singular fiber of an elliptic fibration. This leads to an alternative proof of Kodaira's description of the monodromy around and the behavior of the modulus function near the singular fiber, as given in Table 6.2.40.
- Definition 7.4.3 of the number of k -periodic fibers for α , counted with multiplicities. The computation in (7.5.2) of this number for any element α of the Mordell–Weil group of any elliptic surface with at least one section and at least one singular fiber. The formula is in terms of the number of fixed point fibers for α , which is equal to zero for a QRT automorphism, and the way α permutes the irreducible components of reducible fibers.
- The computation in Corollary 5.1.9 of the action of the QRT automorphism on $H_2(S, \mathbb{Z})$ when no member of the pencil of biquadratic curves in $\mathbb{P}^1 \times \mathbb{P}^1$ contains a horizontal or vertical axis. The fact that in this case the number of k -periodic fibers for the QRT automorphism, counted with multiplicities, is equal to $k^2 - 1$. The characterization in Corollary 5.1.12 of the pencils of biquadratic curves for which the QRT automorphism acts on $H_2(S, \mathbb{Z})$ as an Eichler–Siegel transformation.
- The observation in Section 5.2 that every element of finite order of the Mordell–Weil group of a rational elliptic surface is a Manin QRT automorphism. For each $2 \leq m \leq 6$, the explicit description of the Weierstrass data of the elements of the Mordell–Weil group of order m . The construction of pencils of biquadratic curves with a QRT map of order m in terms of the way the QRT map permutes the irreducible components of the reducible singular fibers.
- The generalization in Sections 6.2–6.4 of the theory of elliptic surfaces to the case that the surface need not be compact. My main motivation for this was to have the validity of a number of basic facts for local models, elliptic fibrations in a tubular neighborhood of a singular fiber. Of course this generalization does not apply to global topological statements in which the compactness of the surface is essential.
- The characterizations in Lemma 7.3.2 and Remark 7.8.5 of the elements of the Mordell–Weil group that act as Eichler–Siegel transformations on the Néron–Severi group.
- The description in Lemma 7.7.3 of the rotation map of an arbitrary element $\alpha \in \text{Aut}(S)_\varphi^+$ of the Mordell–Weil group of any elliptic surface $\varphi : S \rightarrow C$. The description in Lemma 7.7.7 and Corollary 7.7.10 of the asymptotic behavior for $k \rightarrow \infty$ of the set of k -periodic fibers for α .
- The description in Chapter 8 of the behavior of the real period functions and real rotation function of an elliptic fibration with a real structure and a real element α of the Mordell–Weil group, respectively. The description in Lemma 8.1.5 and Corollary 8.4.5 of the asymptotic behavior for $k \rightarrow \infty$ of the set of real k -periodic fibers for α .
- The detailed proof of the various equivalent characterizations of rational elliptic surfaces in Theorem 9.1.3. The statement in Proposition 9.2.10 that an elliptic

surface with the same modulus function and monodromy as a rational elliptic surface is isomorphic to it.

- The various characterizations in Proposition 9.2.22 of the rational elliptic surfaces without reducible fibers. The detailed proof that their isomorphism classes are in bijective correspondence with the isomorphism classes of del Pezzo surfaces of degree one.
- The classification in Proposition 9.2.17 of the rational elliptic surfaces with a nondiscrete automorphism group.
- The analysis in Section 9.2.5 of a pencil of biquadratic curves in $\mathbb{P}^1 \times \mathbb{P}^1$ such that the corresponding rational elliptic surface has the generic configuration of singular fibers $12 I_1$.
- The chaotic nature of the Hesse map from the complex projective line to itself, as formulated in Proposition 11.1.2, and the characterization of the Hesse surface in Proposition 11.1.6.
- The consequences in Proposition 10.1.2 of the condition that the biquadratic curves in the pencil are symmetric, or more generally, that the QRT transformation is the square of an element of the Mordell–Weil group.
- The relation in Section 10.2 between pencils of symmetric biquadratic curves in $\mathbb{P}^1 \times \mathbb{P}^1$ and pencils of quadrics in \mathbb{P}^2 . The ensuing identification in Section 10.3.3 of the QRT root defined by a pencil of symmetric biquadratic curves in $\mathbb{P}^1 \times \mathbb{P}^1$ with the Poncelet mapping when the circumscribed quadrics belong to a pencil of quadrics in \mathbb{P}^2 .
- The identification in Section 11.2 of the billiard map with a Poncelet map, and hence with a QRT root, where the pencil of circumscribed quadrics of the Poncelet mapping is dual to the confocal family of inscribed quadrics for the billiard map.
- The application in sections 11.5–11.7 and 11.4 of the theory to a number of examples from mathematical physics and to the Lyness map, respectively.
- The proof in Section 11.9 that the rational transformation of the plane, introduced by Viallet, Grammaticos, and Ramani [200, Section 2], is not birationally conjugate to a QRT map. On the other hand, since the Weierstrass data of this map are equal to the Weierstrass data of a QRT map, it behaves very much like a QRT map.
- The description in Section 12.1 of the singular fibers that appear after blowing up a singular member of a given pencil of biquadratic curves in $\mathbb{P}^1 \times \mathbb{P}^1$, and the way the QRT automorphism permutes their irreducible components.

Acknowledgments

I thank Theo Tuwankotta, Jan Stienstra, Frans Oort, Frits Beukers, Reinout Quispel, John Roberts, Gert Heckman, Eduard Looijenga, Johan van de Leur, Erik van den Ban, Gunther Cornelissen, Heinz Hanßmann, Luuk Hoevenaars, Claude Viallet, and Alex Quintero Velez for their stimulation and expert help. Special thanks go to Jaap

Eldering, who provided the computer pictures, which in turn prompted me to develop the real aspects of QRT maps in more detail.

J.J. Duistermaat
Mathematisch Instituut, Universiteit Utrecht
January 10, 2010

Note by Johan Kolk

In March 2010 Hans Duistermaat passed away. As always he was actively engaged in research, but an aggressive illness took his life in a short period of just two weeks. By that time the manuscript of this book was completely finished. Ann Kostant, Springer, and Johan Kolk, Utrecht University, saw the book through its final editorial stages before sending it on to production.

Chapter 1

The QRT Map

1.1 The Rational Formula for the QRT Map

In Lemma 1.1.1 below we present the horizontal and vertical switches, defined in Section in terms of a pencil of biquadratic curves, as rational transformations of the plane. For this purpose it is convenient to write a biquadratic polynomial in the form

$$p(x, y) := \sum_{i,j=0}^2 x^{2-i} A_{ij} y^{2-j} = X A Y, \quad (1.1.1)$$

where the coefficients of p are given by a 3×3 matrix $A = (A_{ij})_{i,j=0}^2$. In the shorthand notation $p(x, y) = X A Y$, X and Y denote the row and column vectors with coefficients

$$Y_k := y^{2-k}, \quad X_k := x^{2-k} \quad \text{for } k = 0, 1, 2. \quad (1.1.2)$$

With this notation, we have the following formulas for the QRT map.

Lemma 1.1.1 *Let A^0 and A^1 be two linearly independent 3×3 matrices, and let p^0 and p^1 be the biquadratic polynomials (1.1.1) with A replaced by A^0 and A^1 , respectively. Let ι_1 , ι_2 , and τ be the horizontal switch, the vertical switch, and the QRT map defined by the pencil (0.0.1) of biquadratic curves. Define the vector-valued functions f and g of one variable by*

$$f(y) := (A^0 Y) \times (A^1 Y), \quad g(x) := (X A^0) \times (X A^1). \quad (1.1.3)$$

Then

$$\iota_1(x, y) = (\xi(x, y), y), \quad \text{where } \xi(x, y) = \frac{f_0(y) - f_1(y)x}{f_1(y) - f_2(y)x}, \quad (1.1.4)$$

$$\iota_2(x, y) = (x, \eta(x, y)), \quad \text{where } \eta(x, y) = \frac{g_0(x) - g_1(x)y}{g_1(x) - g_2(x)y}, \quad (1.1.5)$$

and

$$\tau(x, y) = \iota_2(\iota_1(x, y)) = (\xi(x, y), \eta(\xi(x, y), y)). \quad (1.1.6)$$

Proof. We carry out the recipe of Section for the computation of the horizontal switch. If p_z denotes the biquadratic polynomial (1.1.1) with $A = A_z := A^0 - z A^1$, then $p_z(x, y) = a_z(y)x^2 + b_z(y)x + c_z(y)$, where $a_z(y) = (A_z Y)_0$, $b_z(y) = (A_z Y)_1$, and $c_z(y) = (A_z Y)_2$. The horizontal switch of the point (x, y) is equal to (x', y) , where $x' = -x - b_z(y)/a_z(y)$. If (x, y) is not a base point, then we have to substitute in all the formulas the value of z such that (x, y) lies on the curve $p_z(x, y) = 0$, that is, $z = p^0(x, y)/p^1(x, y) = (X A^0 Y)/(X A^1 Y)$. This leads to

$$A_z = A^0 - z A^1 = A^0 - \frac{X A^0 Y}{X A^1 Y} A^1 = \frac{1}{X A^1 Y} ((X A^1 Y) A^0 - (X A^0 Y) A^1),$$

hence $b_z(y)/a_z(y) = \beta/\alpha$, where

$$\begin{aligned} \beta &= (X A^1 Y) (A^0 Y)_1 - (X A^0 Y) (A^1 Y)_1, \\ \alpha &= (X A^1 Y) (A^0 Y)_0 - (X A^0 Y) (A^1 Y)_0. \end{aligned}$$

The coefficients of x^2 , x , and 1 in β are equal to

$$\begin{aligned} (A^1 Y)_0 (A^0 Y)_1 - (A^0 Y)_0 (A^1 Y)_1 &= -f_2(y), \\ (A^1 Y)_1 (A^0 Y)_1 - (A^0 Y)_1 (A^1 Y)_1 &= 0, \end{aligned}$$

and

$$(A^1 Y)_2 (A^0 Y)_1 - (A^0 Y)_2 (A^1 Y)_1 = f_0(y),$$

respectively. The coefficients of x^2 , x , and 1 in α are equal to

$$\begin{aligned} (A^1 Y)_0 (A^0 Y)_0 - (A^0 Y)_0 (A^1 Y)_0 &= 0, \\ (A^1 Y)_1 (A^0 Y)_0 - (A^0 Y)_1 (A^1 Y)_0 &= f_2(y), \end{aligned}$$

and

$$(A^1 Y)_2 (A^0 Y)_0 - (A^0 Y)_2 (A^1 Y)_0 = -f_1(y),$$

respectively. It follows that

$$\begin{aligned} x' &= -x - b_z(y)/a_z(y) \\ &= -x - \beta/\alpha \\ &= -(x^2 f_2(y) - x f_1(y) - x^2 f_2(y) + f_0(y))/(x f_2(y) - f_1(y)) \\ &= (x f_1(y) - f_0(y))/(x f_2(y) - f_1(y)). \end{aligned}$$

The computation of the vertical switch ι_2 is analogous, and the QRT map had been defined in Section as $\tau = \iota_2 \circ \iota_1$. \square

Quispel, Roberts, and Thompson *defined* the QRT map in [168] and [169] by means of the formulas (1.1.6), (1.1.4), (1.1.5). They subsequently proved that ι_1 and

ι_2 leave the biquadratic curves (0.0.1) invariant and therefore are the horizontal and vertical switches as defined in Section . Because ι_1 and ι_2 , and therefore also the QRT map τ , leave each of the biquadratic curves (0.0.1) invariant, they leave the rational function

$$F(x, y) := q^0(x, y)/q^1(x, y) = \frac{X A^0 Y}{X A^1 Y} \quad (1.1.7)$$

invariant. The iterates $(\tau^k)_{k \in \mathbb{Z}}$ are called the *discrete dynamical system* generated by the QRT map, with $k \in \mathbb{Z}$ as the discrete time. It follows that F is an *integral* of the discrete dynamical system $(\tau^k)_{k \in \mathbb{Z}}$ in the sense that F is invariant under all the transformations τ^k , $k \in \mathbb{Z}$. For this reason $(\tau^k)_{k \in \mathbb{Z}}$ is called an *integrable discrete dynamical system*.

By definition, $\tau = \iota_2 \circ \iota_1$, where ι_1 and ι_2 are involutions; hence $\tau^{-1} = \iota_1 \circ \iota_2 = \iota_1 \circ \tau \circ \iota_1^{-1} = \iota_2 \circ \tau \circ \iota_2^{-1}$. This implies that for each $k \in \mathbb{Z}$, both ι_1 and ι_2 conjugate τ^k with τ^{-k} . One says in this situation that the discrete dynamical system defined by the QRT map is *time reversible*, with each of the involutions ι_1 and ι_2 of the plane acting as a time-reversing transformation.

Roberts and Quispel [175, Appendix A] observed that the area form

$$\omega := \frac{1}{X A^1 Y} dx \wedge dy \quad (1.1.8)$$

is invariant under the QRT transformation τ . Here the denominator $Z A^1 Y$ could have been replaced by any of the biquadratic polynomials $z_0 p^0(x, y) + z_1 p^1(x, y)$. The corresponding invariance of the dual two-vector fields w such that $\omega \cdot w = 1$ follows from our Corollary 3.4.4. In summary, the QRT map is time-reversible, integrable, and area-preserving.

Finally Quispel, Roberts, and Thompson showed in [168] and [169] that quite a large number of rational transformations of the plane that occur in mathematical physics are QRT maps. Also for other examples from the literature, such as the elliptic billiard (Section 11.2) and the Lyness map (Section 11.4), it was a nontrivial discovery that these fit into the framework of QRT maps.

1.2 Indeterminacy of the QRT Map

In [168], [169] it is not mentioned whether the map acts on the real or the complex plane, although all the pictures are in the real plane. We will work in the complex plane in order to obtain more uniform results. For instance, a polynomial of degree d has d complex zeros when counted with multiplicities, whereas in the real domain d would only be an upper bound for the number of zeros. Also, complex projective algebraic manifolds often are nonempty and connected, whereas their real parts may be empty or have several connected components. The presentation of the map τ as a rational mapping from the affine plane to itself has several defects, even if we

work over the complex numbers. The same can be said about the presentation of the integral F as a rational function on the affine plane.

First, a rational function $r(x, y) = n(x, y)/d(x, y)$ of two variables becomes infinite at every point where $d(x, y) = 0$ and $n(x, y) \neq 0$. When this happens for one of the coordinates of $\tau(x, y)$, then for the iteration of τ we need to know the image of these points at infinity under the mapping τ , which is not given by the expressions in (1.1.4), (1.1.5). In our presentation of the QRT map in Chapter 3 we will resolve this by viewing both x and y as coordinates of a point on the complex projective line $\mathbb{P}^1 = \mathbb{C} \cup \{\infty\}$, where the infinite image point becomes a well-defined finite point in the Cartesian product $\mathbb{P}^1 \times \mathbb{P}^1$ of the two complex projective lines.

A more serious defect is that at the points (x_0, y_0) where both the denominator and the numerator vanish, that is, where $d(x_0, y_0) = n(x_0, y_0) = 0$, the value of $r(x, y)$ is completely undetermined, in the sense that for any complex number c there exist points (x, y) arbitrarily close to (x_0, y_0) such that $d(x, y) \neq 0$ and $r(x, y) = c$. More precisely, for the given c the equation $n(x, y) - c d(x, y) = 0$ defines an algebraic curve C_c in the plane on which $r(x, y) = c$, and all the curves $C_c, c \in \mathbb{C}$, run through the same point (x_0, y_0) .

The same problem occurs for the invariant rational function (1.1.7), where the common zeros (x_0, y_0) of the denominator and the numerator of F are the points (x_0, y_0) that lie on every member of the pencil of biquadratic curves (0.0.1). Such a point (x_0, y_0) is called a *base point* of the pencil (0.0.1), and we will see in Lemma 3.1.1 that, counted with multiplicities, there are eight base points in $\mathbb{P}^1 \times \mathbb{P}^1$. This implies that there is always at least one base point in $\mathbb{P}^1 \times \mathbb{P}^1$, whereas for generic pencils of biquadratic curves there are eight distinct base points. Therefore the problem of indeterminacy will always occur if one works in the complex space $\mathbb{P}^1 \times \mathbb{P}^1$, but often it will also happen at real points. In our presentation of the QRT map in Chapter 3 we will resolve the indeterminacies by passing to a complex two-dimensional manifold S on which the members of the pencil are separated from each other, basically by adding the parameter z in (0.0.2) as a tag to the variables.

1.3 Reconstruction

In this section we discuss the problem of finding explicit computational procedures to determine, for an arbitrary birational transformation τ of the plane, whether it is a QRT map and, if so, to find coefficient matrices A^0 and A^1 such that τ is equal to the QRT map defined by A^0 and A^1 . We start with a reduction to a problem in fewer variables.

Because any linearly independent pair of linear combinations of A^0 and A^1 defines the same QRT map, it is the two-dimensional linear subspace spanned by A^0 and A^1 that has to be determined from τ , rather than the matrices themselves. For an n -dimensional vector space E , let $G_2(E)$ denote the *Grassmann manifold* of all two-dimensional linear subspaces of E . If $L \in G_2(E)$, then for each basis e_1, e_2 of L the two-vector $w = e_1 \wedge e_2$ is a nonzero element of $\Lambda^2 E$ of rank equal to two.

Let w be any element of $\Lambda^2 E$. Then w will be identified with the linear mapping $\epsilon \mapsto i_\epsilon w : E^* \rightarrow E$, and the rank of w is defined as the dimension of the linear subspace $L = w(E^*)$ of E . There exist $k \in \mathbb{Z}$ such that $0 \leq 2k \leq n$ and linearly independent elements e_j , $1 \leq j \leq 2k$, in E such that $w = e_1 \wedge e_2 + e_3 \wedge e_4 + \cdots + e_{2k-1} \wedge e_{2k}$. Because $i_\epsilon(a \wedge b) = \epsilon(a)b - \epsilon(b)a$ for every $\epsilon \in E^*$ and $a, b \in E$, it follows that $w(E^*)$ is equal to the linear span of the e_j , $1 \leq j \leq 2k$, and $\text{rank } w = 2k$. On the other hand, the k -fold wedge product w^k of w with itself is equal to $k! e_1 \wedge e_2 \wedge e_3 \wedge e_4 \wedge \cdots \wedge e_{2k-1} \wedge e_{2k} \neq 0$, whereas $w^{k+1} = 0$, and therefore k is also equal to the maximal nonnegative integer l such that $w^l \neq 0$, where $w^0 := 1$. In particular, the set $(\Lambda^2 E)_2$ of all rank-2 elements of $\Lambda^2 E$ is equal to the set of all $w \in \Lambda^2 E$ such that $w \neq 0$ and $w \wedge w = 0$.

Let $P(\Lambda^2 E)$ denote the space of all one-dimensional linear subspaces of $\Lambda^2 E$, which is isomorphic to the m -dimensional projective space \mathbb{P}^m , with $m = (n(n-1)/2) - 1$. Let $P((\Lambda^2 E)_2)$ denote the set of all one-dimensional linear subspaces of $\Lambda^2 E$ that are contained in $(\Lambda^2 E)_2$. Then there is a unique mapping $\iota : P((\Lambda^2 E)_2) \rightarrow G_2(E)$ such that $w(E^*) = \iota(l)$ whenever $l \in (\Lambda^2 E)_2$ and $w \in l$. Furthermore, ι is an isomorphism from $P((\Lambda^2 E)_2)$ onto $G_2(E)$. The inverse of ι is given by the condition that $\iota(l) = L$ if and only if $e_1 \wedge e_2 \in l$ for all $e_1, e_2 \in L$ if and only if l is the span of $e_1 \wedge e_2$ for any basis e_1, e_2 of L .

For $n = \dim E = 4$, $\dim \Lambda^2 E = 4 \cdot 3/2 = 6$, hence $P(\Lambda^2 E) \simeq \mathbb{P}^5$. Furthermore, $\dim \Lambda^4 E = 1$, and the equation $w \wedge w = 0$ identifies $P((\Lambda^2 E)_2)$ with a quadric hypersurface in \mathbb{P}^5 . It was the idea of Plücker [163] to identify the projective lines in \mathbb{P}^3 , that is, the elements of $G_2(E)$, with the elements of the quadric hypersurface in $P(\Lambda^2 E)$ defined by the equation $w \wedge w = 0$. For arbitrary finite-dimensional vector spaces, the mapping $\mathbb{C}e_1 + \mathbb{C}e_2 \mapsto \mathbb{C}e_1 \wedge e_2 : G_2(E) \rightarrow P(\Lambda^2 E)$ is called the *Plücker embedding*. The linear coordinates on $\Lambda^2 E$ are called the *Plücker coordinates* on $G_2(E)$, and the equation $w \wedge w = 0$ the *Plücker equation*. Because $G_2(E)$ is a smooth manifold of dimension $2(n-2)$, the solution set in $\Lambda^2 E \setminus \{0\}$ of the equation $w \wedge w = 0$ is a smooth manifold of dimension $2(n-2) + 1$. It follows that if $n > 4$, there are dependencies between the $\binom{n}{4}$ quadratic equations $(w \wedge w)_j = 0$ for w .

In our situation, E is equal to the nine-dimensional vector space of all 3×3 -matrices. The vector-valued functions $f(y)$ and $g(x)$ in (1.1.3) are polynomials in y and x of degree ≤ 4 ,

$$f_k(y) = \sum_{l=0}^4 f_{kl} y^{4-l}, \quad g_k(x) = \sum_{l=0}^4 g_{kl} x^{4-l}, \quad k = 0, 1, 2. \quad (1.3.1)$$

Each of the $2 \cdot 3 \cdot 5 = 30$ coefficients f_{kl}, g_{kl} depends in an antisymmetric bilinear way on (A^0, A^1) , and therefore is a linear function of the element $A^0 \wedge A^1 \in \Lambda^2 E$, the ‘‘Plücker coordinate’’ of the two-dimensional vector space spanned by A^0 and A^1 . Let A_{ij} be the $(3i + j + 1)$ th coordinate of the element $A \in E$, and let e_k , $1 \leq k \leq 9$, denote the standard basis of E with respect to these coordinates. Then the $e_k \wedge e_l$ with $1 \leq k < l \leq 9$ form a basis of $\Lambda^2 E$, where $\dim \Lambda^2 E = 36$.

The first test for τ to be a QRT map as in (1.1.6) is that its first coordinate has to be of the form $\xi(x, y)$ as in (1.1.4). This function determines the horizontal switch ι_1 , and then the second test for τ is whether $\iota_2 = \tau \circ \iota_1$ is a vertical switch as in (1.1.5). The functions $\xi(x, y)$ and $\eta(x, y)$ in (1.1.4) and (1.1.5) determine the respective vector-valued functions function $f(y)$ and $g(x)$ up to a constant scalar multiple, and the third test for τ is whether these are polynomial functions of degree ≤ 4 . The elements of $\Lambda^2 E$ that yield (1.1.3) with f and g replaced by αf and βg , respectively, are the

$$w = \alpha u + \beta v + \sum_{i=1}^6 c_i n_i,$$

where

$$\begin{aligned} u &= f_{00} e_4 \wedge e_7 + (f_{01}/2) (e_4 \wedge e_8 + e_5 \wedge e_7) + f_{02} e_5 \wedge e_8 \\ &\quad + (f_{03}/2) (e_5 \wedge e_9 + e_6 \wedge e_8) + f_{04} e_6 \wedge e_9 - f_{10} e_1 \wedge e_7 \\ &\quad - (f_{11}/2) (e_1 \wedge e_8 + e_2 \wedge e_7) - f_{12} e_2 \wedge e_8 - (f_{13}/2) (e_2 \wedge e_9 + e_3 \wedge e_8) \\ &\quad - f_{14} e_3 \wedge e_9 + f_{20} e_1 \wedge e_4 + (f_{21}/2) (e_1 \wedge e_5 + e_2 \wedge e_4) \\ &\quad + f_{22} e_2 \wedge e_5 + (f_{23}/2) (e_2 \wedge e_6 + e_3 \wedge e_5) + f_{24} e_3 \wedge e_6, \\ v &= g_{00} e_2 \wedge e_3 + (g_{01}/2) (e_2 \wedge e_6 - e_3 \wedge e_5) + g_{02} e_5 \wedge e_6 \\ &\quad + (g_{03}/2) (e_5 \wedge e_9 - e_6 \wedge e_8) + g_{04} e_8 \wedge e_9 - g_{10} e_1 \wedge e_3 \\ &\quad - (g_{11}/2) (e_1 \wedge e_6 - e_3 \wedge e_4) - g_{12} e_4 \wedge e_6 - (g_{13}/2) (e_4 \wedge e_9 - e_6 \wedge e_7) \\ &\quad - g_{14} e_7 \wedge e_9 + g_{20} e_1 \wedge e_2 + (g_{21}/2) (e_1 \wedge e_5 - e_2 \wedge e_4) \\ &\quad + g_{22} e_4 \wedge e_5 + (g_{23}/2) (e_4 \wedge e_8 - e_5 \wedge e_7) + g_{24} e_7 \wedge e_8, \end{aligned}$$

$n_1 = e_4 \wedge e_9 + e_6 \wedge e_7 - 2 e_5 \wedge e_8$, $n_2 = e_1 \wedge e_8 - e_2 \wedge e_7 - 2 e_4 \wedge e_5$, $n_3 = e_2 \wedge e_9 + e_3 \wedge e_8 - 2 e_5 \wedge e_6$, $n_4 = e_1 \wedge e_6 + e_3 \wedge e_4 - 2 e_2 \wedge e_5$, $n_5 = e_3 \wedge e_7 - e_2 \wedge e_8 + e_4 \wedge e_6$, and $n_6 = e_1 \wedge e_9 - e_2 \wedge e_8 - e_4 \wedge e_6$. The fourth and final test for τ is whether there exist $\alpha \neq 0$, $\beta \neq 0$, and c_j , $1 \leq j \leq 6$, such that the rank of w is equal to two, that is, $w \wedge w = 0$. These are $\binom{9}{4} = 126$ quadratic equations for the eight unknowns α , β , and c_j , $1 \leq j \leq 6$. I have not tried to find the explicit equations and inequalities for the f_{kl} and g_{kl} such that these equations have a solution $\alpha \neq 0$ and $\beta \neq 0$. On the other hand, if w corresponds to such a solution, then $w(E^*)$ is the two-dimensional space of coefficient matrices of the sought-for biquadratic polynomials.

A complication that occurs in quite a number of the explicit examples in the literature is that the polynomials $f_0(y)$, $f_1(y)$, $f_2(y)$ in (1.1.3) have a common strictly positive degree, which is divided out in (1.1.4). That is, the horizontal switch may have degree $d_1 < 4$; see Definition 5.1.3. In this case the common factor is one of the unknowns in the problem.

There are special cases in which the reconstruction is straightforward. For instance, if τ is a QRT map, then each point of indeterminacy of ι_1 or ι_2 is a base point of the pencil of biquadratic curves. If these points of indeterminacy can be explicitly determined, then the vanishing of a biquadratic polynomial p at these points is a system of as many linear equations for p as the number of points of indeterminacy. If

this system of equations determines a two-dimensional vector space P of biquadratic polynomials, then we only need to check whether the mapping τ is equal to the QRT map defined by P .

Another case in which the reconstruction is explicit is for QRT roots of pencils of symmetric biquadratic curves; see Section 10.1.1. A case in which the reconstruction is very straightforward is for McMillan maps, see Section 11.5.

A quite different question is whether there are some general principles behind the fact that so many rational transformations of the plane that come from mathematical physics are QRT maps.

Chapter 2

The Pencil of Biquadratic Curves in $\mathbb{P}^1 \times \mathbb{P}^1$

In many of the examples of QRT maps in the literature, see Chapter 11, one is interested in the action of the iterates of the mapping in the real affine plane. However, as mentioned in Section 1.2, the results are much more uniform if the field \mathbb{R} is replaced by its algebraic closure \mathbb{C} , and the complexified affine plane is compactified to the Cartesian product of two complex projective lines. The point is that in the complex projective setting, the full force of complex projective algebraic geometry is at our disposal. If the objects are defined over \mathbb{R} , then the real objects will be studied as the fixed-point sets in the complex manifolds of a complex conjugation, an involution that acts on tangent spaces as complex antilinear mappings.

A natural generalization of complex algebraic geometry is complex analytic geometry, and we will freely use the terminology of the latter. Our background reference for algebraic geometry in a complex analytic setting is the book of Griffiths and Harris [74]. More algebraically oriented, and working over more general fields than only the field of complex numbers, are Hartshorne [80] and Shafarevich [182]. In Sections 2.1 and 2.2 we introduce some of the definitions and notation that will be used throughout this book. These sections have grown into the present size in order to serve as a reasonably complete source of references. At a first reading of this book these sections may be skipped, and then consulted when referred to.

In Section 2.3 we discuss the basic properties of elliptic curves. In Section 2.4 we show that every smooth biquadratic curve is an elliptic curve, and compute, among others, the coefficients g_2 and g_3 of its Weierstrass normal form as explicit polynomial expressions in the coefficients of the biquadratic polynomial. In Section 2.5 we prove that the QRT map acts as a translation on the elliptic curve, and compute, in the Weierstrass normal form, the coordinates of the image point under the QRT map of the point at infinity, again as explicit polynomial expressions in the coefficients of the biquadratic polynomial. In Section 2.5.2 we apply this to pencils of biquadratic curves, whereas Section 2.5.3 is an exposition of the Picard–Fuchs equations for one-parameter families of Weierstrass curves, due to Bruns and Manin. Some real aspects of the above topics are discussed in Section 2.6